ANALYSIS OF SAMPLING PATTERN AND LUMA-CHROMA FILTER DESIGN FOR SUBPIXEL-BASED IMAGE DOWNSAMPLING

Jin Zeng, Oscar C. Au, Yuanfang Guo, Jiahao Pang, Ketan Tang, Yonggen Ling

Department of Electronic and Computer Engineering,
Hong Kong University of Science and Technology, Hong Kong.
E-mail: {jzengab, eeau, eeandyguo, jpang, tkt, ylingaa}@ust.hk

ABSTRACT

Subpixel-based image downsampling is attractive in that it produces higher apparent resolution of down-sampled images on LCD displays. However increased luminance resolution is achieved at the price of color fringing artifacts. In this paper, we propose an algorithm to find a pleasing balance between increased resolution and color fidelity. We separate the subpixel-based downsampling into two stages, shifting followed by downsampling with anti-aliasing filtering. In stage one, we find special characteristics of the luminance and chrominance spectra of the shifted image, based on which the optimal sampling pattern is found. In stage two, anti-aliasing filters for luminance and chrominance are designed respectively. Experimental results verify that the proposed method manages to suppress color artifacts while maintaining high luminance sharpness.

Index Terms— Frequency-domain analysis, image downsampling, subpixel rendering, color fringing

1. INTRODUCTION

For patterned displays like color LCD displays, a pixel is composed of several color elements emitting the primary colors red, green and blue. These elements are called subpixels and they fuse together to appear as a single color to human eyes [1, 2, 3, 4]. So there is a chance to gain apparent resolution by individually controlling the subpixel values but at the price of color fringing artifact [5, 6, 7, 8]. "Clear Type" is a subpixel-based font display technology announced by Microsoft in 1998 that improves the readability of small text on LCD displays [9]. Fig. 1 illustrates that subpixel rendering ("Clear Type") reduces staircase artifacts on edges effectively and reconstructs the shape information with higher fidelity than pixel-based rendering.

In this paper we focus on image downsampling using subpixel rendering technology for RGB stripe displays. Downsampling is required when low resolution display is used to display high resolution images/videos. For pixel-based methods, a simple one called Direct Pixel-based Downsampling (DPD) performs downsampling by selecting one out of every N pixels [10]. Severe aliasing occurs as shown in Fig. 2(b) for DPD. Another method called Pixel-based Downsampling with Anti-aliasing Filter (PDAF) [10] eliminates the aliasing at the price of blurring the image. By taking into account the subpixel arrangement in LCD displays, Daly *et al.* proposed a downsampling pattern in [11] which is referred to as Direct Subpixel-based Down-sampling (DSD) [10] as shown in Fig. 2(c) and it achieves higher sampling frequency than DPD from signal point of view, but suffers from color artifacts. More general studies of subpixel-based downsampling patterns are investigated in [12, 13].

Fig. 1. Rendering 'm': left to right, 'm' in italic, pixel-based rendering with jagged edges, subpixel rendering with smooth edges.

Previous methods investigate the filter design for suppressing annoying artifacts. In [14] Platt proposed a set of filters based on an error metric derived from psychophysical experiments, which was extended to font display in [15]. Kim proposed a filter design method based on a virtual image model [16]. However these methods make the image blurred. Fang *et al.* proposed methods MMSE-SD [17], DSD-FA and DDSD-FA [10] which achieve high sharpness in downsampled images however color artifacts are noticeable especially in sharp edge regions. Following Fang's work, Tang *et al.* proposed methods DDSDFA-CR and DDSDFA-CB [18] to reduce color artifacts, but the methods either blur the image or do not remove the artifacts sufficiently. Therefore existing subpixel-based methods are not satisfying. In this paper, we attempt to balance the luminance sharpness and color fidelity. We examine the subpixel-based downsampling process by separating it into two stages, shifting followed by downsampling with anti-aliasing filtering. It is found that the color artifact is introduced after shifting so we suggest chroma filtering after shifting and before downsampling which is never

978-1-4799-2893-4/14/$31.00 ©2014 IEEE

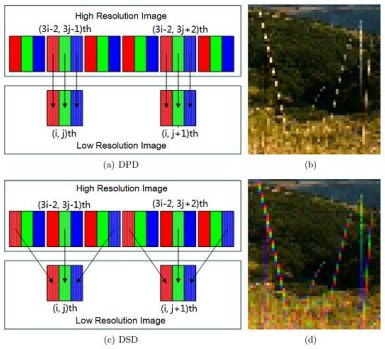

Fig. 2. (a)DPD. (b) Magnified result of DPD with aliasing artifacts on grass. (c)DSD. (d)Magnified result of DSD with smooth grass but color artifacts.

proposed in previous work. Similar to [10], the analysis of aliasing effect is performed in frequency-domain, based on which an optimal sampling pattern is found. In addition, we propose an algorithm to find the optimal cut-off frequency of the filters for luma and chroma components.

The rest of the paper is organized as follows: In Section 2 we find the optimal sampling pattern and design the luma-chroma filters. In Section 3 experiments are performed to verify that the proposed method achieves good performance in reducing color artifacts while retaining sharpness. Section 4 concludes the paper.

2. PROPOSED DOWNSAMPLING METHOD

2.1. Optimal Sampling Pattern

Without loss of generality, we consider downsampling the original image L of size $M \times N$ to a small image S of size $m \times n$, where $M = 3m$, $N = 3n$. If $M \neq 3m$ or $N \neq 3n$, use conventional pixel-based downsampling methods (e.g. bicubic) to resize L to be $3m \times 3n$ first. Let $(R(i,j), G(i,j), B(i,j))$ represent red, green, and blue component values at the (i,j)th pixel in L.

The subpixel-based downsampling can be accomplished by first shifting the color components according to sampling patterns, and then apply the pixel-based downsampling with anti-aliasing filtering. For example, DSD can be done by shifting the red component to the right by one pixel, and blue to the left by one pixel, followed by DPD.

The shifted image is denoted by L' and RGB values at (i,j)th pixel is denoted as $(R'(i,j), G'(i,j), B'(i,j))$. Let (m_k, n_k) ($k = 1,2,3$ represents R, G and B) be the sampling locations of RGB components for 3:1 downsampling, i.e., $m_k, n_k \in \{-1, 0, 1\}$ for each 3×3 block. So we have,

$$\begin{cases} R'(i,j) &= R(i+m_1, j+n_1) \\ G'(i,j) &= G(i+m_2, j+n_2) \\ B'(i,j) &= B(i+m_3, j+n_3), \end{cases} \tag{1}$$

In order to analyze the behavior of luminance and chrominance components, we convert the RGB image into YUV space [19] using the transformation matrix in (2).

$$\begin{pmatrix} Y \\ U \\ V \end{pmatrix} = \begin{pmatrix} 0.30 & 0.59 & 0.11 \\ -0.17 & -0.33 & 0.50 \\ 0.50 & -0.42 & -0.08 \end{pmatrix} \begin{pmatrix} R \\ G \\ B \end{pmatrix}. \tag{2}$$

The Fourier transform of the luminance component is

$$\begin{aligned} \hat{Y}'(u,v) &= 0.30\hat{R}'(u,v) + 0.59\hat{G}'(u,v) + 0.11\hat{B}'(u,v) \\ &= 0.30\hat{R}(u,v)e^{j2\pi\varphi_1} + 0.59\hat{G}(u,v)e^{j2\pi\varphi_2} \\ &\quad + 0.11\hat{B}(u,v)e^{j2\pi\varphi_3}, \end{aligned} \tag{3}$$

where $\varphi_k = m_k u + n_k v$, $k = 1,2,3$.

Each color component such as $\hat{G}$ can be decomposed into low-frequency part $\hat{G}_l$ and high frequency part $\hat{G}_h$, i.e., $\hat{G} = \hat{G}_l + \hat{G}_h$, and due to the high correlations among R, G and B components, the high frequency parts of RGB tend to be similar[20], i.e., $\hat{G}_h \approx \hat{R}_h \approx \hat{B}_h$. Hence we have,

$$\hat{Y}'_h(u,v) = \hat{G}_h(u,v)\left(0.30e^{j2\pi\varphi_1} + 0.59e^{j2\pi\varphi_2} + 0.11e^{j2\pi\varphi_3}\right). \tag{4}$$

The error introduced during the downsampling is due to aliasing in the high frequency part, so the energy of high frequency is measured as follows,

$$\begin{aligned} E_{Y'_h}(u,v) &= \hat{Y}'_h(\hat{Y}'_h)^* \\ &= \hat{G}'_h(\hat{G}'_h)^*(0.4502 + 0.354\cos 2\pi(\varphi_1 - \varphi_2) + \\ &\quad 0.066\cos 2\pi(\varphi_1 - \varphi_3) + 0.1293\cos 2\pi(\varphi_3 - \varphi_1)) \\ &= \hat{G}'_h(\hat{G}'_h)^* C_{Y'_h}(u,v), \end{aligned} \tag{5}$$

where $C_{Y'_h}(u,v)$ is the coefficient independent of input image signal. So to minimize the high frequency energy we can instead minimize the coefficient. Moreover, the frequency component along horizontal and vertical axes catches more attention thus we focus on the analysis on the axes. By setting $v = 0$, we have,

$$\begin{aligned} C_{Y'_h}(u,0) &= 0.4502 + 0.354\cos 2\pi(m_1 - m_2)u \\ &\quad + 0.066\cos 2\pi(m_1 - m_3)u + 0.1293\cos 2\pi(m_3 - m_1)u. \end{aligned} \tag{6}$$

Similarly we have the coefficients for chrominance components of high frequency,

$$\begin{aligned} C_{U'_h}(u,0) &= 0.3878 + 0.1122\cos 2\pi(m_1 - m_2)u \\ &\quad - 0.17\cos 2\pi(m_1 - m_3)u - 0.33\cos 2\pi(m_3 - m_1)u, \end{aligned} \tag{7}$$

$$\begin{aligned} C_{V'_h}(u,0) &= 0.4328 - 0.42\cos 2\pi(m_1 - m_2)u \\ &\quad - 0.08\cos 2\pi(m_1 - m_3)u + 0.0672\cos 2\pi(m_3 - m_1)u. \end{aligned} \tag{8}$$

Fig. 3 shows the frequency spectra of luminance and chrominance of the original and the shifted image. Luminance for the shifted image turns out to be more compact than the original one, which means that high frequency is canceled, but chrominance appears spread and high frequency value is enlarged. It is advantageous for luminance since less aliasing will occur during downsampling, however for chrominance

it is the opposite. That is why color artifact is noticeable in subpixel rendering images. Hence the objective is to find a sampling pattern that minimizes the high frequency energy for both luminance and chrominance. Since the downsampling ratio is 3:1, we take the integral from $1/6$ to $1/2$, where aliasing occurs, as the high frequency energy amount. Note that optimal solutions are different for minimizing the energy of luminance and chrominance, therefore we need to find a trade-off between luma aliasing and color artifact. In light of this we instead minimize the positive weighted sum of the luminance and chrominance energy,

$$\min_{m_k} \int_{\frac{1}{6}}^{\frac{1}{2}} \left(wC_{Y_h'}(u,0) + \frac{1-w}{2} \left(C_{U_h'}(u,0) + C_{V_h'}(u,0) \right) \right) \mathrm{d}u \tag{9}$$

$$\text{s.t.} \quad m_k \in \{-1,0,1\}, k = 1,2,3,$$

where w is a positive weighting factor affected by sensitivity to luminance and chrominance error, and different w will result in different optimal solutions. Without further information and preference of luma or chroma aliasing effects, we treat luma and chroma error equally, thus we set $w = 0.5$, and the optimal solution is $(m_1 - m_2, m_1 - m_3) = (\pm 1, 0)$. If w is large enough i.e. $w = 1$ such that high sharpness is favored, the optimal solution is $(m_1 - m_2, m_1 - m_3) = (\pm 1, \pm 2)$. And small w i.e. $w \leq 0.25$ results in $(m_1 - m_2, m_1 - m_3) = (0,0)$ where no color distortion is tolerated. And $(m_1 - m_2, m_1 - m_3) = (\pm 1, 0)$ is a good compromise between the two extreme cases according to our experiments.

Similarly we can get the optimal solution for n_1, n_2, n_3. However due to the RGB vertical stripe subpixel arrangement on LCD panels, i.e., $n_1 \leq n_2 \leq n_3$, the optimal solution becomes $(n_1 - n_2, n_1 - n_3) = (-1, -2)$, i.e., $(n_1, n_2, n_3) = (-1, 0, 1)$. Since two spectra are considered equal if one of them can be obtained from the other via flipping, we can let $(m_1, m_2, m_3) = (-1, 0, -1)$ without loss of generality. At this point, the optimal solution is reached, and the frequency spectra in Fig. 3 are obtained via optimal sampling pattern.

2.2. Luma-Chroma Anti-aliasing Filter Design

To prevent aliasing in downsampling, low-pass filter with Nyquist cut-off frequency should be applied to original image [21]. However as seen in Section 2.1, magnitudes of horizontal and vertical aliasing spectra for luminance are smaller in subpixel-based downsampling than in DPD, so the horizontal and vertical cut-off frequency, f_Y^h and f_Y^v can be extended beyond 1/6 to retain more signal details. For chrominance, cut-off frequencies $f_U^h, f_U^v, f_V^h, f_V^v$ should be suppressed to reduce color distortion. Downsampling of shifted image via optimal sampling pattern with anti-aliasing filtering respectively for luma and chroma, is called SD-LCAF, which stands for Subpixel-based Downsampling with Luma-Chroma Anti-aliasing Filter. As pointed out in [22], the probability density function of spectral energy for natural images can be modeled as Laplacian distribution. We can thus represent the normalized spectrum $\hat{Y}$ using a zero-mean

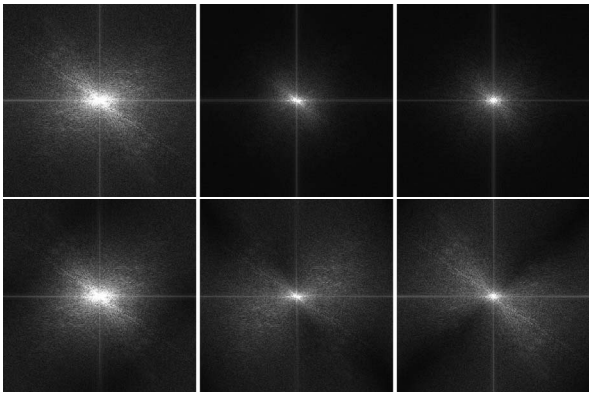

Fig. 3. Frequency spectral of original and shifted image based on optimal sampling pattern(top to down: original and shifted; left to right: Y, U and V; the image is lena)

circularly symmetric Laplacian model with variance $2\lambda_Y^2$, i.e., $\hat{Y}/E_Y \sim (1/2\lambda_Y)\exp(-|f|/\lambda_Y)$ where E_Y is the total energy of $\hat{Y}$. In the proposed SD-LCAF, we choose f_Y^h, f_Y^v to make the aliasing amount of subpixel-based method equal to that of pixel-based method. The aliasing amount is measured by integrating the aliasing spectrum energy from 0 to the cut-off frequency. Thus we have,

$$\int_0^{f_n} \frac{E_\Omega}{2\lambda_\Omega} \exp \frac{-|f-1/3|}{\lambda_\Omega} \mathrm{d}f = \int_0^{f_\Omega^H} \frac{E_\Omega'}{2\lambda_{\Omega'}} \exp \frac{-|f-1/3|}{\lambda_\Omega'} \mathrm{d}f, \tag{10}$$

where f_n is the Nyquist frequency which is 1/6 in this case, E_Ω is the total spectrum energy of the original image with Laplacian model $\{0, \lambda_\Omega\}$, E_Ω' is for shifted image spectrum with Laplacian model $\{0, \lambda_\Omega'\}$, $\Omega \in Y, U, V$. So f_Ω^H can be calculated, and due to symmetry $f_\Omega^V = f_\Omega^H$. And results show that for Y the cut-off frequency can be extended beyond Nyquist frequency, but suppressed for U and V.

3. EXPERIMENTAL RESULTS

The goal of the method is to maintain apparent luminance resolution, while reducing color artifacts. To compare with the existing methods, two measurements are adopted as follows.

LSM(Luminance Sharpness Measure) [10]: since the major resolution difference of various methods occurs in high frequency details, LSM is defined as the average of directional high-frequency energy, i.e.,

$$LSM(X) = \frac{1}{4} \sum_{k=1}^{4} \parallel H^k * X \parallel_1, \tag{11}$$

where $H^k = [1 \; -1]$, $k = 1,2,3,4$ for horizontal, vertical, diagonal and antidiagonal directions. Larger LSM value indicates higher apparent resolution.

CDM(Color Distortion Measure) [10]: PDAF has negligible color distortion according to observation and is taken as

Fig. 4. Test images. Left to right: baboon, cartoon, cathedral, chart, fonts, lena, trees, window.

Table 1. LSM of the test images.

Image	SD-LCAF	DDSD-FA	DSD-FA	PDAF
baboon	0.98	0.97	0.90	0.80
cartoon	1.39	1.41	1.45	1.42
cathedral	0.95	0.94	0.90	0.79
chart	0.95	0.95	0.88	0.81
fonts	0.96	0.95	0.91	0.86
lena	1.18	1.14	0.99	0.99
trees	0.97	0.97	0.90	0.83
window	1.05	1.04	0.96	0.84
average	1.05	1.05	0.99	0.92

the reference to compute PSNR_U and PSNR_V for any image x to be measured,

$$\text{PSNR}_U = 10 \times \lg \frac{255^2}{\text{MSE}_U} \tag{12}$$

$$\text{MSE}_U = \frac{1}{MN}(\| U_x - U_{\text{PDAF}} \|_2^2), \tag{13}$$

where U_x and U_{PDAF} are the U components of x and PDAF respectively. So larger PSNR_U indicates less color distortion. PSNR_V is defined similarly.

Test images are shown in Fig. 4. We simulate the proposed method SD-LCAF compared with PDAF which is pixel-based, and DSD-AF, DDSD-AF [10] which are state-of-art subpixel-based methods. The results are shown in Table 1 for LSM and Table 2 for CDM. Since the PSNR_U and PSNR_V results are similar, only PSNR_U values are presented. It can be seen that the sharpness of SD-LCAF is as high as DDSD-FA, and higher than those of DSD-FA and PDAF. Moreover, the PSNR_U values of SD-LCAF are higher than those of DSD-FA and DDSD-FA, indicating that SD-LCAF greatly suppresses the color artifacts.

Subjective results are illustrated in Fig. 5. It is verified that SD-LCAF produces similar images as DDSD-FA and DSD-FA in that these three methods achieve higher sharpness than PDAF due to subpixel-based processing. Besides, unlike DDSD-FA or DSD-FA, SD-LCAF does not contain noticeable color artifacts on edges in the regions framed by the red rectangles. Another example of font image in Fig. 6 depicts the comparison between DDSD-FA and SD-LCAF, which shows that SD-LCAF effectively reduces color errors while maintaining high resolution.

Table 2. PSNR_U of the test images.

Image	SD-LCAF	DDSD-FA	DSD-FA
baboon	36.62	26.50	30.54
cartoon	39.14	31.70	35.56
cathedral	34.28	26.92	28.52
chart	35.56	25.22	29.03
fonts	31.78	23.74	25.99
lena	38.51	30.70	32.99
trees	35.64	27.09	30.88
window	35.37	28.09	32.04
average	35.86	27.50	30.70

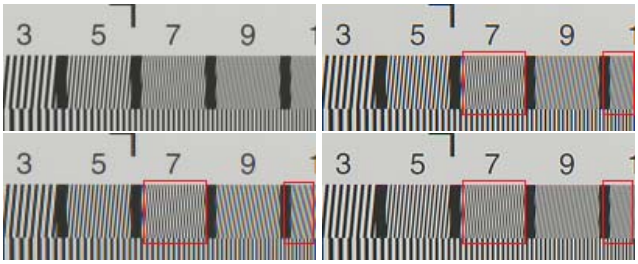

Fig. 5. Subjective results. Left to right, then top to bottom: PDAF, DDSD-FA, DSD-FA, SD-LCAF.

4. CONCLUSION

By separating the subpixel-based downsampling into two stages, shifting and downsampling with anti-aliasing filtering, the proposed SD-LCAF successfully reduces the color artifacts and the sharpness is retained. Based on the analysis of the luminance and chrominance components of the shifted image in frequency domain, we propose the optimal sampling pattern in terms of balancing the sharpness and color fidelity. The anti-aliasing filters for luma and chroma are designed respectively based on the characteristics of the energy distribution. Experiments verify that the proposed method provides superior results than existing subpixel or pixel-based downsampling methods.

5. ACKNOWLEDGEMENT

This work is supported in part by Research Grants Council of HKSAR, China (GRF Project No. 610109 and 610112).

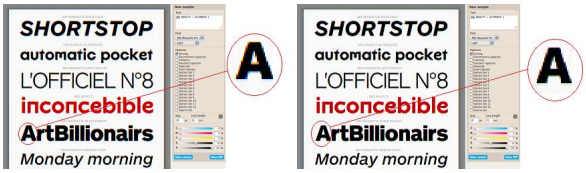

Fig. 6. Comparison of down-samped images using DDSD-FA and SD-LCAF. Left: DDSD-FA, right: SD-LCAF.

6. REFERENCES

[1] S.Gibson, "Sub-pixel font rendering technology," https://www.grc.com/default.htm.

[2] Li-Ming Chen and Shin Hasegawa, "Influence of pixel-structure noise on image resolution and color for matrix display devices," *Journal of the Society for Information Display*, vol. 1, no. 1, pp. 103–110, 1993.

[3] Lu Fang, O.C. Au, and Ngai-Man Cheung, "Subpixel rendering: from font rendering to image subsampling [applications corner]," *Signal Processing Magazine, IEEE*, vol. 30, no. 3, pp. 177–189, May 2013.

[4] Lu Fang, O.C. Au, Yi Yang, Weiran Tang, and Xing Wen, "Subpixel-based image downsampling-some analysis and observation," in *Multimedia and Expo, 2009. ICME 2009. IEEE International Conference on*, June 2009, pp. 1576–1577.

[5] Lu Fang and Oscar C Au, "Subpixel-based image downsampling with min-max directional error for stripe display," *Selected Topics in Signal Processing, IEEE Journal of*, vol. 5, no. 2, pp. 240–251, 2011.

[6] Michiel A Klompenhouwer, Gerard Haan, and Rob A Beuker, "13.4: Subpixel image scaling for color matrix displays," in *SID Symposium Digest of Technical Papers*. Wiley Online Library, 2002, vol. 33, pp. 176–179.

[7] Ketan Tang, Oscar C Au, Lu Fang, Zhiding Yu, and Yuanfang Guo, "How anti-aliasing filter affects image contrast: An analysis from majorization theory perspective," in *Multimedia and Expo (ICME), 2011 IEEE International Conference on*. IEEE, 2011, pp. 1–6.

[8] D.S. Messing and S. Daly, "Improved display resolution of subsampled colour images using subpixel addressing," in *Image Processing. 2002. Proceedings. 2002 International Conference on*, 2002, vol. 1, pp. I–625–I–628 vol.1.

[9] Miscrosoft, "Cleartype information," http://research.microsoft.com/en-us/projects/cleartype.

[10] Lu Fang, Oscar C Au, Ketan Tang, and Aggelos K Katsaggelos, "Antialiasing filter design for subpixel downsampling via frequency-domain analysis," *Image Processing, IEEE Transactions on*, vol. 21, no. 3, pp. 1391–1405, 2012.

[11] Scott J Daly and Rajesh Reddy K Kovvuri, "Methods and systems for improving display resolution in images using sub-pixel sampling and visual error filtering," Aug. 19 2003, US Patent 6,608,632.

[12] Yonggen Ling, Oscar C Au, Ketan Tang, Jiahao Pang, Jin Zeng, and Lu Fang, "An analytical study of subpixel-based image down-sampling patterns in frequency domain," in *Visual Communications and Image Processing (VCIP), 2013*. IEEE, 2013, pp. 1–6.

[13] Lu Fang, Oscar C Au, Jingjing Dai, Hanli Wang, and Ngai-Man Cheung, "Analytical study of rgb vertical stripe and rgbx square-shaped subpixel arrangements," in *Image Processing (ICIP), 2012 19th IEEE International Conference on*. IEEE, 2012, pp. 333–336.

[14] John C Platt, "Optimal filtering for patterned displays," *Signal Processing Letters, IEEE*, vol. 7, no. 7, pp. 179–181, 2000.

[15] Claude Betrisey, James F Blinn, Bodin Dresevic, Bill Hill, Greg Hitchcock, Bert Keely, Don P Mitchell, John C Platt, and Turner Whitted, "20.4: Displaced filtering for patterned displays," in *SID Symposium Digest of Technical Papers*. Wiley Online Library, 2000, vol. 31, pp. 296–299.

[16] Jun-Seong Kim and Chang-Su Kim, "A filter design algorithm for subpixel rendering on matrix displays," in *Proc. 15th European Signal Processing Conf.(EUSIPCO)*, 2007, pp. 1487–1491.

[17] Lu Fang, Oscar C Au, Ketan Tang, Xing Wen, and Hanli Wang, "Novel 2-d mmse subpixel-based image downsampling," *Circuits and Systems for Video Technology, IEEE Transactions on*, vol. 22, no. 5, pp. 740–753, 2012.

[18] Ketan Tang, Oscar C Au, Lu Fang, Yuanfang Guo, and Jiahao Pang, "Chroma replacing and adaptive chroma blending for subpixel-based downsampling," in *Multimedia Signal Processing (MMSP), 2013 IEEE 15th International Workshop on*. IEEE, 2013, pp. 212–217.

[19] ITU, "Recommendation itu-r bt.601-5," 1995.

[20] Nai-Xiang Lian, Lanlan Chang, Yap-Peng Tan, and Vitali Zagorodnov, "Adaptive filtering for color filter array demosaicking," *Image Processing, IEEE Transactions on*, vol. 16, no. 10, pp. 2515–2525, 2007.

[21] Rafael C Gonzalez and Richard E Woods, "Digital image processing, 2nd," *SL: Prentice Hall*, 2002.

[22] Edmund Y Lam and Joseph W Goodman, "A mathematical analysis of the dct coefficient distributions for images," *Image Processing, IEEE Transactions on*, vol. 9, no. 10, pp. 1661–1666, 2000.